FULL PAPER

# Modeling Polymer Dielectric/Pentacene Interfaces: On the Role of Electrostatic Energy Disorder on Charge Carrier Mobility

By *Nicolas G. Martinelli, Matteo Savini, Luca Muccioli, Yoann Olivier, Frédéric Castet, Claudio Zannoni, David Beljonne,* and *Jérôme Cornil**

**Force-field and quantum-chemical calculations are combined to model the packing of pentacene molecules at the atomic level on two polymer dielectric layers (poly(methyl methacrylate) (PMMA) versus polystyrene (PS)) widely used in field-effect transistors and to assess the impact of electrostatic interactions at the interface on the charge mobility values in the pentacene layers. The results show unambiguously that the electrostatic interactions introduce a significant energetic disorder in the pentacene layer in contact with the polymer chains; a drop in the hole mobility by a factor of 5 is predicted with PS chains while a factor of 60 is obtained for PMMA due to the presence of polar carbonyl groups.**

## 1. Introduction

The field of organic electronics has developed tremendously over the last twenty years.[1] The key advantages of organic semiconductors compared to their inorganic equivalents are the versatility of chemical synthesis, the ease of processing (in particular over large areas), and low production costs. Among the numerous applications, organic field-effect transistors (OFETs) are attractive devices planned to be used as building blocks in low-cost electronic components.[2–5] The optimization of their performance requires the improvement of the charge transport properties in organic layers that are quantified by the charge carrier mobility value ($\mu$).[6] FETs based on amorphous silicon yield mobilities around 1 $cm^2 V^{-1} s^{-1}$ while intensive research has now led to values as high as 30 $cm^2 V^{-1} s^{-1}$ for organic materials in the best cases.[7]

In spite of good device performance, a complete understanding of charge transport in organic semiconductors at the microscopic level is still lacking. A hopping regime, in which charges jump from molecule to molecule, is typically assumed to describe charge transport in bulk disordered systems where static positional disorder (giving rise to a distribution of electronic couplings between the interacting units) and energetic disorder (giving rise to a distribution of energies for the transport levels, that is, the HOMO level in the case of hole transport, as a result of fluctuations in the nature of the molecular environment around each unit) promote charge localization over individual molecules.[8] Similarly, recent theoretical studies have also suggested that the charges become strongly localized in highly ordered systems such as molecular crystals due to thermal fluctuations and the resulting dynamic energetic and/or spatial disorder.[9–11] In OFETs, the charge transport mostly operates (at low bias) within the first molecular layer in contact with the insulator layer.[3,12] The transport properties, and hence the charge mobility values, are thus expected to be further affected in the conducting channel by

i) the electrostatic properties of the insulator layer. A significant drop of the mobility by up to one order of magnitude was reported in OFETs based on polytriarylamine chains when replacing low-k polymer dielectrics by poly(methyl methacrylate) (PMMA).[13] Similar observations were made in the case of pentacene layers.[14,15] This deterioration of the mobility was attributed to an increase in the energetic disorder promoted by the polar carbonyl bonds of the PMMA chains.[13] This model is consistent with previous theoretical studies of charge transport in solids formed by molecules bearing a permanent dipole moment.[16] Shifts of the threshold voltages in OFETs upon different surface treatment of the gate insulator have also been explained on the same basis.[17,18] In the case of highly polarizable dielectric layers, the formation of Frölich polarons has been suggested, implying that the drift of the charges is slowed by the nuclear polarization of the dielectric layer.[19] However, this model does not appear to be applicable for polymer dielectrics.[20,21]

ii) the morphology of the interfacial organic layer promoted by the dielectric substrate. The formation of grain boundaries in the conducting channel is one of the major structural

[*] Dr. J. Cornil, N. G. Martinelli, Dr. Y. Olivier, Dr. D. Beljonne
Laboratory for Chemistry of Novel Materials
University of Mons
Place du Parc 20, Mons, 7000 (Belgium)
E-mail: jerome@averell.umh.ac.be
M. Savini, Dr. L. Muccioli, Prof. C. Zannoni
Dipartimento di Chimica Fisica e Inorganica and INSTM
Università di Bologna
Viale Risorgimento 4, Bologna, 40136 (Italy)
Dr. F. Castet
Institut des Sciences Moléculaires, UMR CNRS 5255
Université de Bordeaux
351 Cours de la Libération, Talence, 33405 (France)

DOI: 10.1002/adfm.200901077

limitations to high charge mobility values.[5,22,23] Recent studies on OFETs based on pentacene show that the grain size varies as a function of the nature of the polymer dielectrics and that the carrier mobility is very sensitive to the grain size below a root-mean-square value of about 0.8 μm.[14,24] The viscoelasticity of the polymer chains, and hence the deposition temperature, may also influence the charge mobility.[14,25]

iii) the interaction with electronic states at the surface. Organic semiconductors typically display a p-type behavior when using $SiO_2$ as the dielectric layer in FETs due to the presence of electron traps on the surface.[15,26] These chemical traps can be eliminated by using polymer dielectrics[26] or by treatment of the $SiO_2$ surface.[15,27] Correlations between cleaning techniques and OFET electrical characteristics have been clearly established.[28]

Since many parameters are likely to modulate the transport properties in OFET experiments and since the impact of a given factor is generally difficult to extract from experimental measurements, theoretical calculations can prove very useful by shedding light on these effects, as illustrated by recent phenomenological models addressing the role of electrostatic interactions between the semiconducting and dielectric layers.[20] However, studies involving an atomic description of the system[29,30] have not been reported so far to the best of our knowledge. Accordingly, we have combined in the present work molecular dynamics (MD) simulations to establish the organization at the atomic scale of pentacene molecules on polymer dielectrics and quantum-chemical calculations to assess the actual impact of electrostatic interactions on the charge mobility values.

We focus here on pentacene molecules (i.e., one of the most studied and efficient organic semiconductors) deposited on top of polystyrene (PS) versus PMMA chains, widely used as polymer dielectrics. This choice is motivated by the fact that PS is nonpolar while PMMA features polar bonds associated to the carbonyl groups. Moreover, the performance of OFETs involving these interfaces have been assessed.[14,15]

In a way similar to the experimental fabrication of an OFET,[31] we obtained with atomic MD simulations 3D periodic cells consisting of a polymer (PS or PMMA)/pentacene wafer equilibrated at 300 K. Each slab is about 60-Å thick, allowing for the generation of two independent dielectric/pentacene interfaces with the organic semiconductor forming four homeotropically oriented crystalline layers (Fig. 1). Note that the finite size of the supercell (60 × 60 Å) does not allow us to describe morphological defects such as grain boundaries.

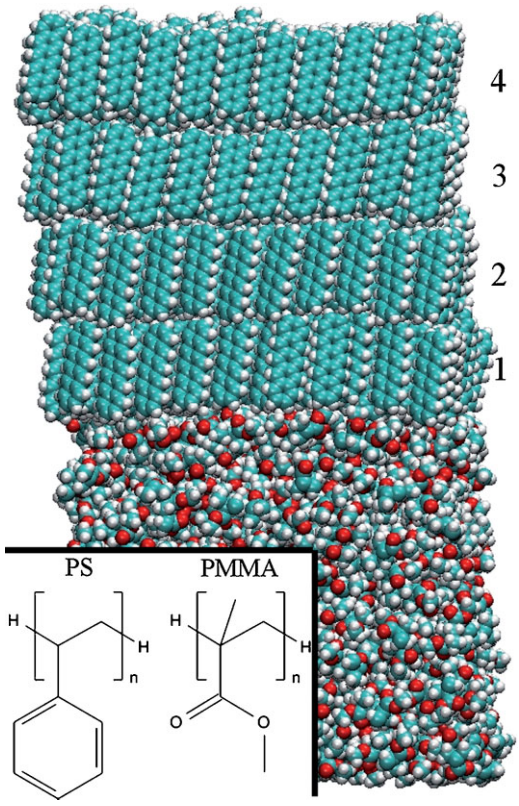


**Figure 1.** Atomic description of the pentacene/PMMA dielectric interface. The inset shows the chemical structures of the two polymers dielectrics studied.

## 2. Results and Discussion

### 2.1. Energetic Disorder

The rate of charge hopping between two adjacent molecules is affected by the energetic disorder, that is, the energy difference between the initial state $P1^+$ P2 and the final state P1 $P2^+$ differing by the transfer of a hole (+) from a pentacene molecule P1 to a pentacene molecule P2. For transport in the channel of OFETs, two different factors contribute to the energy difference between the initial and final states (that we refer to here as the total energetic disorder). The first ($\Delta E_{\text{diel}}$) accounts for the changes in the electrostatic interactions between the pentacene molecules and the dielectric layer going from the initial to the final state; these changes primarily originate from the fact that the interaction between the charge on a given pentacene molecule and the charge distribution in the dielectric layer does depend on the actual location of the charge in the channel (i.e., on the molecule onto which the charge sits) due to the amorphous nature of the polymer substrate. In order to evaluate this contribution at the atomic level, we have calculated the Coulomb interaction between the charge distribution of the neutral molecule and that of the dielectric layer ($E^0$) and between the charge distribution of the charged pentacene molecule and the dielectric layer ($E^+$) in the initial state (i). A similar procedure has to be repeated for the final state (f) following the transfer of the hole from molecule 1 to 2. On that basis, $\Delta E_{\text{diel}}$ is defined as

$$\Delta E_{\text{diel}} = (E_{\text{diel}})_{\text{f}} - (E_{\text{diel}})_{\text{i}} = (E_1^0 + E_2^+) - (E_1^+ + E_2^0) \quad (1)$$

These Coulomb energies were calculated from atomic point charges obtained with density functional theory (DFT) calculations at the B3LYP//aug-cc-pVDZ level and interatomic distances within the minimum image convention.[32] Note that i) we do not account

for the possible energetic disorder induced by the slight positional disorder in the simulated pentacene layer since our primary focus is to determine the way the charge transport properties are affected by the introduction of the dielectric layer; ii) since the Coulomb forces are dominated by the interactions between a pentacene molecule and the nearest repeat units of the polymer chains due to the amorphous nature of the dielectric layer,[20] the use of a macroscopic dielectric constant is not appropriate at such short distances and has therefore been omitted when calculating the $\Delta E_{\text{diel}}$ parameters;[33] and iii) the impact of dynamic electronic polarization effects associated to a reorganization of the electronic density of the pentacene molecules in the presence of the polymer dielectrics is found to be limited due to the low polarizability of the saturated polymer chains in the dielectric layer, as supported by the quantum-chemical calculations reported later. The second contribution giving to rise energetic disorder ($\Delta E_{\text{field}}$) is due to the presence of an external electric field when applying a bias between the source and drain electrodes of the FET.[34] At low bias, the electric field is homogeneous along the channel and introduces an energy gradient of the transport levels (i.e., in the energy of the HOMO levels of the individual molecules). The $\Delta E_{\text{diel}}$ and $\Delta E_{\text{field}}$ contributions are added to define the total energetic disorder $\Delta E_{\text{tot}}$ associated to the hopping process:[35,36]

$$\Delta E_{\text{tot}} = \Delta E_{\text{field}} + \Delta E_{\text{diel}} = e\vec{F}\vec{d} + (E_{\text{diel}})_{\text{f}} - (E_{\text{diel}})_{\text{i}} \quad (2)$$

where $e$ is the charge, $F$ the electric field, and $d$ the distance between molecules.

Figure 2 displays the distribution of $\Delta E_{\text{diel}}$ for all pairs of pentacene molecules in the different layers on top of PMMA versus PS, as averaged over 100 snapshots extracted every 100 ps from a MD run of 10 ns; the averaging procedure is justified by the fast lattice dynamics yielding a fast saturation of the width of energetic disorder, as illustrated in Figure S2 of the Supporting Information. The distributions are symmetric with respect to zero since each molecule is considered at the same time as a possible initial or final site; all distributions can be fitted with a Gaussian distribution. For each polymer dielectric, the broadening is the most pronounced in the layer in direct contact with the polymer chains. The standard deviation $\sigma$ of the Gaussian distribution as a function of the distance $z$ from the interface can be fitted by a $1/z$ function (see Fig. S1 of the Supporting Information), as expected from Coulomb law. When comparing the two polymers, the main difference is observed in the surface layer where $\sigma_{\text{PMMA}} \approx 2\sigma_{\text{PS}}$. From a simple qualitative reasoning, we thus expect that the charge transport properties within the pentacene surface layer (i.e., in contact with the polymer) should be significantly affected, with a lower mobility predicted for PMMA.

### 2.2. Polarization versus Electrostatic Effects

The impact of electronic polarization effects induced by the dielectric layer on the energetic disorder has been estimated using a mixed Valence-Bond/Hartree–Fock (VB/HF) approach.[37] This approach is based on the semi-empirical Hartree–Fock Austin Model 1 (AM1) method and involves fragment orbitals that can be relaxed in a controlled way. The extent of polarization effects can be assessed by comparing the magnitude of the Coulomb interactions at the interface with and without electronic relaxation effects in the molecular orbitals. We have made this comparison in the case of PS where we expect the largest polarization effects due to the presence of polarizable benzene units. To do so, a configuration of the pentacene/PS interface has been modified to retain only the benzene rings in the dielectric layer due to computational limits. The system subjected to the quantum-chemical approach is finally made of a single pentacene molecule (neutral or charged) on top of the benzene units lying within a distance of 20 Å (Fig. 3, top), and similar results were obtained for larger cut-off distances. The $\Delta E_{\text{diel}}$ distribution was calculated with Equation 1 by considering all pairs of adjacent pentacene molecules in the layer in contact with the dielectrics (layer 1). The resulting distributions shown in Figure 3 (middle and bottom) demonstrate that the difference between the non-relaxed and relaxed systems is small and hence that the impact of dynamic polarization effects is weak.

### 2.3. Charge Carrier Mobilities

Next, the impact of the polymer dielectrics on transport properties has been assessed quantitatively by propagating charge carriers within a hopping regime in the different pentacene layers by means of kinetic Monte Carlo simulations, with an explicit account of the electrostatic interactions between the pentacene molecules and the polymer chains. The kinetic Monte Carlo technique, originally introduced by Gillespie for studying chemical reactions,[38,39] has recently been successfully used to compute charge mobility values in supramolecular assemblies.[34,40–42] The use of a hopping model is validated by the fact that OFETs typically operate at room temperature or higher, that is, in conditions where thermal disorder favors charge localization.[9] The latter is further reinforced by the energetic disorder created by the electrostatic interactions. We emphasize that we are primarily interested here by the changes in the mobility values induced by the presence of the dielectric layer rather than by the absolute values of the mobility, which are dictated by the amplitude of the relevant molecular parameters defined later. Figure 4 shows the polar plot of the mobility values obtained for the different pentacene layers (with the charge constrained to remain in the same layer) in presence of PMMA versus PS chains. These plots are generated by rotating the direction of the external electric field (with a typical amplitude of $10^4$ V cm$^{-1}$) within the layer in order to explore the anisotropy of charge transport. For each polar angle, the mobility has been calculated for 100 different layer geometries (by extracting a configuration every 100 ps of a total MD run of 10 ns) before getting averaged; the same time-averaged values of $\Delta E_{\text{diel}}$ have been used in all simulations. The trends observed for the mobility reflect the distributions obtained for the $\Delta E_{\text{diel}}$ values. For layers 2 to 4, the influence of the dielectrics on the mobility values is very small, as supported by the narrow energetic distributions. On the contrary, the mobility is significantly lowered in the surface layer (1) due to the increased energetic disorder. We stress that similar mobility values are obtained for the isolated surface layer and for bulk pentacene, thus demonstrating that the drop in the mobility cannot be attributed to changes in the molecular packing at the interface. The mobility is found to be reduced by a factor of 60 for PMMA and 5 for PS compared to bulk

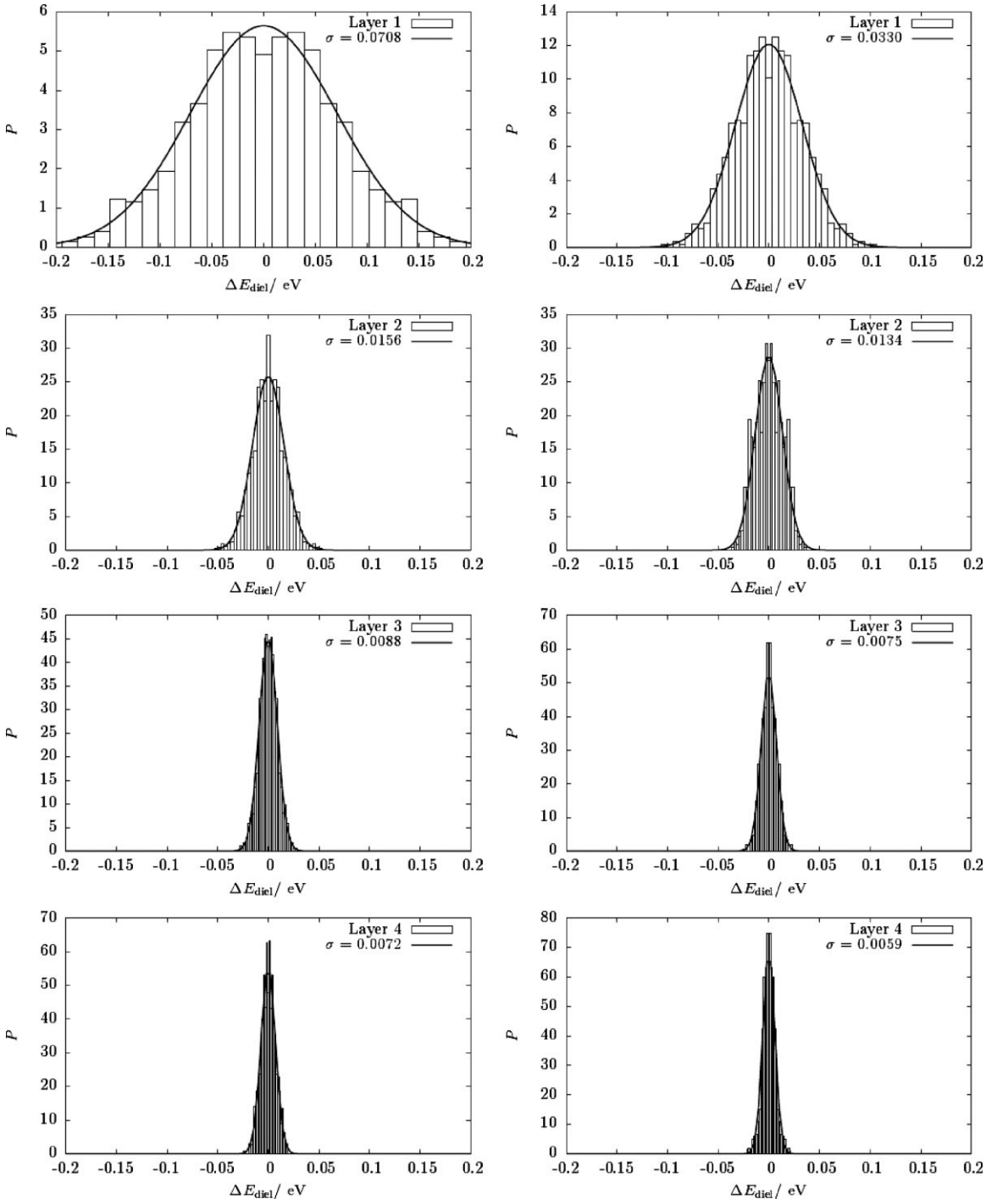


**Figure 2.** Distribution of the site energy difference $\Delta E_{diel}$ in the four pentacene layers in presence of PMMA (left) and PS (right). A fit with a Gaussian distribution is done in each case (the corresponding standard deviation is given). The labeling of the layers is given in Figure 1.

pentacene. The calculated ratio of 12 between PMMA and PS is larger than the reported experimental values on the order of 4.[14,15] However, it is worth recalling that our simulations do not take into account any macroscopic morphological defects such as grain boundaries that are likely to affect the experiment measurements; it has been shown for instance that using PS chains of different molecular weight yields various grain sizes and different mobility values.[14] Similar mobility values are found for PS and PMMA when propagating a hole in the surface layer of the second interface generated with the periodic boundary conditions.

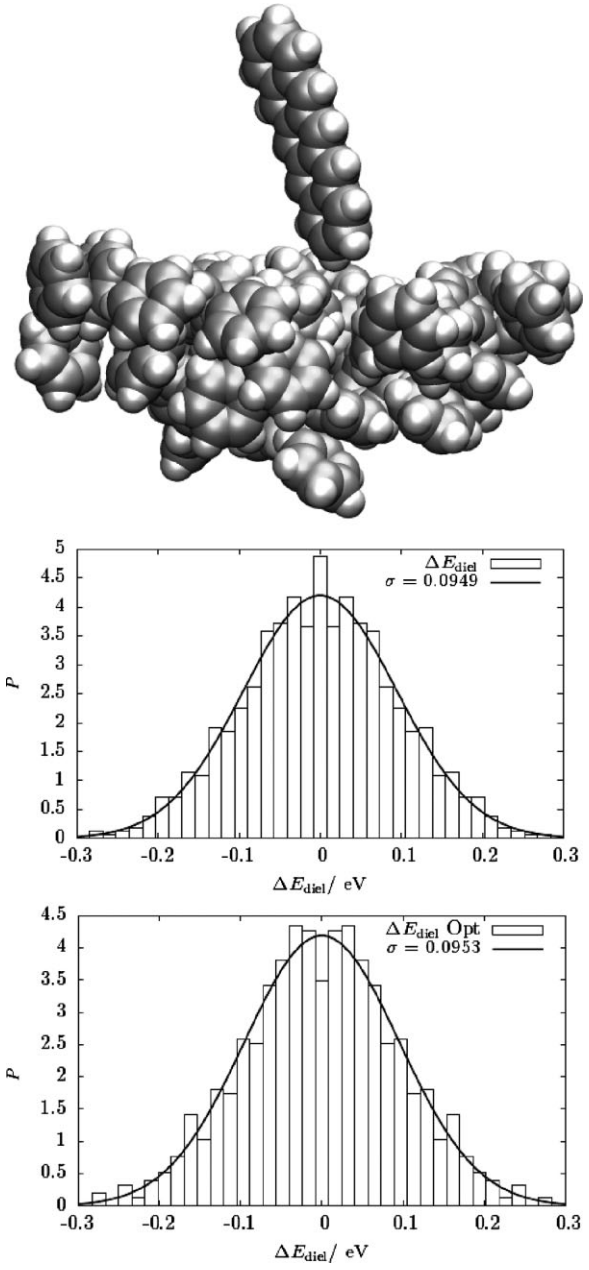


**Figure 3.** Top) Model pentacene/PS interface where each monomer unit has been replaced by a benzene molecule. Middle and bottom) Distribution of $\Delta E_{\rm diel}$ in a layer of pentacenes on top of polarizable benzene units for non-relaxed (middle) and relaxed (bottom) molecular orbitals.

## 3. Conclusions

In summary, we have combined classical and quantum-chemical calculations to model at the atomic level the interface between pentacene layers and a dielectric layer made of either PMMA or PS chains in relation to their use in OFETs. Our calculations demonstrate univocally that the polarity of the polymer chains increases the amount of energetic disorder in the organic semiconducting layer. However, this effect is only pronounced within the surface layer and rapidly decays in the subsequent layers. These findings indicate that the choice of the chemical nature of polymer dielectrics is critical for the optimization of charge transport properties in OFETs.

## 4. Experimental

*Parameterization of the Force Field*: Atomic simulations [43] are nowadays capable of correctly reproducing or even predicting the morphology and physical properties of crystals [44], liquid crystals [29,30,45], polymers [46,47], and biomolecules [48], provided that the force-field empirical parameters, which are used in the potential energy function, are properly derived and validated through the comparison with experimental data [30,48]. Here, in order to obtain the atomic charges required to properly describe the electrostatic properties of the polymers, we first optimized isotactic quaterstyrene and quarter(methyl methacrylate) at the semi-empirical Hartree–Fock AM1 (Austin Model 1) level using Gaussian03 [49]; this method provides reliable molecular geometries [50] that are used to compute the electrostatic potential fitting charges (ESP [51]) at the DFT level (using the B3LYP functional and the aug-cc-pVDZ basis set) with the option Dipole (so that the charges also reproduce the dipole moment of the molecule). Charges on each type of atom in the different monomers were averaged with the constraint of having a zero total charge per monomer and a zero charge on the terminal hydrogen atoms. At the B3LYP/aug-cc-pVDZ level, the permanent dipoles of the monomer are estimated to be 4.6 D and 4.3 D for MMA and 0.4 D and 0.2 D for styrene in the saturated (with a C=C double bond) and unsaturated forms (with C−C single bond and valences saturated with two hydrogen atoms), respectively. The pentacene charges were calculated at the same DFT level starting from the X-ray crystalline geometry downloaded from the Cambridge Crystallographic Data Centre; charges were subsequently symmetrized according to the point group of the molecule. The resulting atomic charges were plugged into the AMBER94 molecular mechanics force field [52] used in all MD simulations following a well-tested methodology that ensures a good accuracy for organic and biological molecules [53,54].

*Packing of the Polymer Chains*: Monomers of PMMA and PS in the reacted form (without terminal hydrogens) were first connected to obtain 50-monomer-long linear isotactic chains (molecular weight: $M_{\rm PMMA} = 5007.7\ {\rm g\ mol^{-1}}$, $M_{\rm PS} = 5209.2\ {\rm g\ mol^{-1}}$). Each chain was replicated 27 times in a cubic lattice to give a starting simulation box with a low density (20 304 atoms for PMMA, 21 654 atoms for PS); similar sample sizes and chain lengths have been demonstrated to be sufficient for reproducing experimental glass transition temperatures with MD simulations [55]. The boxes were first equilibrated at 500 K (i.e., well above the glass transition temperature and close to the melting point), which generates a box size of about 65 Å, then used as input configurations for further runs at progressively lower temperatures until room temperature is reached (300 K) by steps of 25 K. All simulations were done with the Orac MD program [56] in the isothermal–isobaric (NPT) ensemble at atmospheric pressure, with velocity scaling thermostat, isotropic box changes [57] and 3D periodic boundary conditions (PBC) [32,43]. A maximum integration time step of 10 fs was used in a multiple-time-step Scheme [56] for a total equilibration time of at least 10 ns for each temperature. Long-range electrostatic interactions were dealt with the smooth particle mesh Ewald technique [58] with a $40 \times 40 \times 40$ mesh.

*Packing of Pentacene Molecules*: Crystalline pentacene is known to exhibit different polymorphs depending on growing conditions: two bulk-phase crystalline structures exist [59,60] and several thin-film structures have been reported, of which at least two do not coincide with the bulk structures [61,62]. Here we chose the most common bulk crystal polymorph, often termed "vapor" since it is grown from a vapor phase [60], as a starting geometry for our simulations. For sake of illustration, we

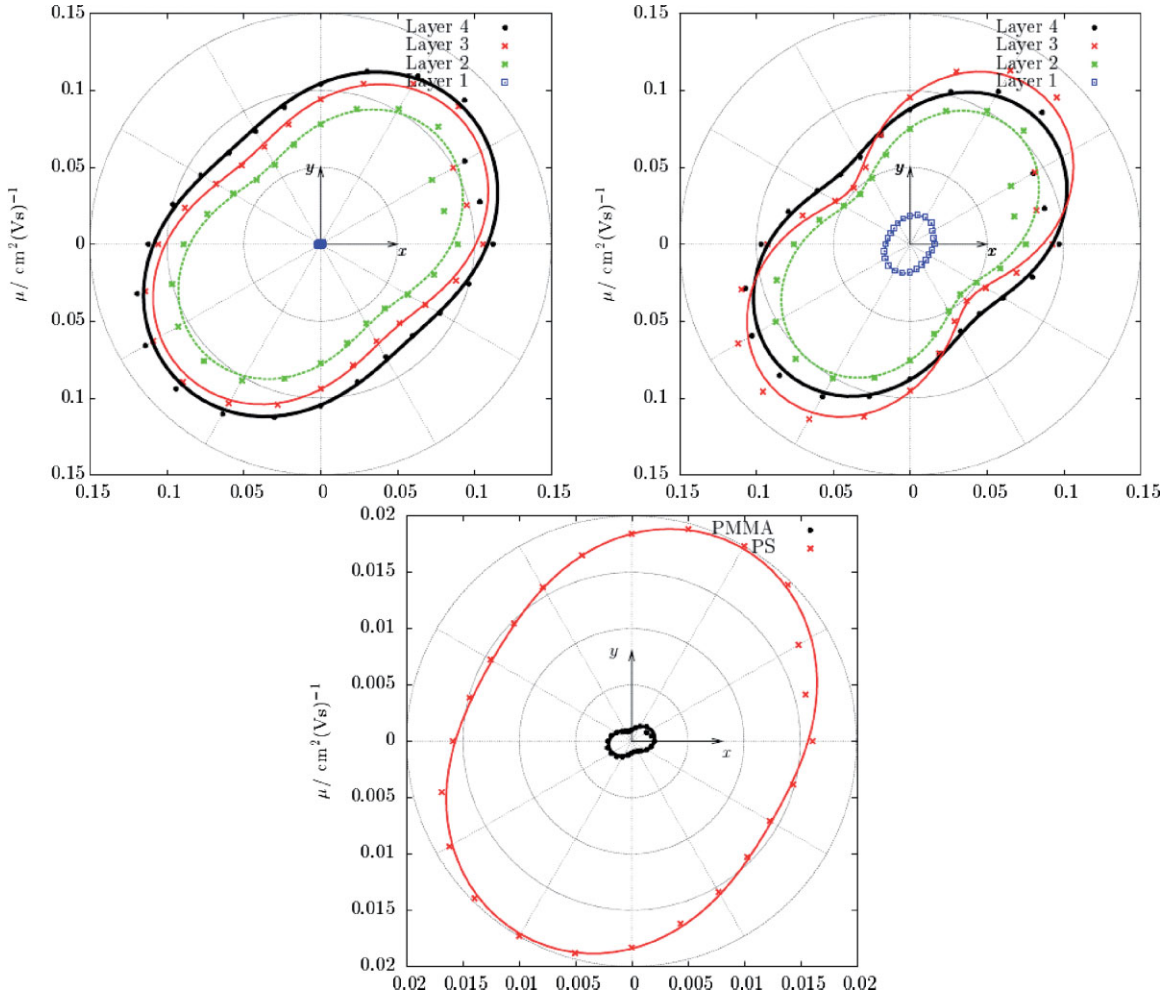


**Figure 4.** Polar plots of the mobility calculated for the four pentacene layers in presence of PMMA (top left) and PS (top right); bottom) zoomed-in layer 1 for both polymers. In each plot, the radius corresponds to the mobility value and the angle to the electric-field orientation.

report in Table 1 the lattice parameters of pentacene single crystals grown from solution versus vapor. A crystalline pentacene sample was built by replicating the experimental crystal unit cell ($Z = 2$) $10 \times 8 \times 2$ times in the *x*, *y*, *z* directions to give a total number of 320 molecules. The number of replica in the *xy* plane was chosen in order to obtain a layer of approximately the same dimension as the polymer box. The initial configuration was submitted to a MD run of 5 ns at room temperature and atmospheric pressure and by imposing an orthorhombic cell by a suitable thermostat [57]. This simulation demonstrates that the crystalline structure is well preserved at room temperature and is similar to the experimental and theoretically predicted [63] unit cell (see Table 1). The adopted force field is thus adequate in this context.

*Sample Preparation*: In a second stage, four equilibrated pentacene layers were added on top of PMMA and PS samples at $T = 300$ K. To do so, bulk samples with 3D periodic boundary conditions (PBCs) were transformed into 2D samples by artificially enlarging the polymer box by 100 Å in the *z* direction in order to generate two vacuum/polymer interfaces. These samples were equilibrated for about 1 ns at constant volume to let dangling chains collapse on the surface before the insertion of pentacene in the box. 3D PBCs were then restored so as to generate two independent polymer dielectric/pentacene interfaces. Afterwards, a pressure of 100 atm was imposed to speed the compression in further MD simulations in the NPT ensemble with a triclinic cell for pentacene [57]. As soon as the pentacene/polymer interface appeared to be sufficiently smooth, the pressure was restored to 1 atm and equilibration and production runs were performed at 300 K during 10 ns to produce the morphologies required for the charge transport simulations (Fig. 1).

**Table 1.** Comparison of the unit cell properties for the "solution" [59] and "vapor" [60] polymorph of pentacene. We also report the results from the present MD simulations based on $10 \times 8 \times 2$ replicas of the experimental unit cell [60] as well as the theoretical predictions by quasi-harmonic lattice dynamics simulations [63].

| Polymorph properties | Solution [59] | Vapor [60] | Vapor, simulation [this work] | Vapor, simulation [63] |
|---|---|---|---|---|
| density [g cm$^{-3}$] | 1.336 | 1.35 | 1.334 | 1.36 |
| *a* [Å] | 6.06 | 6.253 | 6.29 | 5.986 |
| *b* [Å] | 7.90 | 7.786 | 7.81 | 7.776 |
| *c* [Å] | 14.88 | 14.511 | 14.6 | 14.949 |
| $\alpha$ [deg] | 97.90 | 76.65 | 76.65 | 79.45 |
| $\beta$ [deg] | 98.49 | 87.50 | 87.50 | 84.17 |
| $\gamma$ [deg] | 93.49 | 84.60 | 84.61 | 85.71 |
| *T* [K] | 295 | 293 | 298 | 293 |

*Charge Mobility Values*: The transfer rate $k_{if}$ between the initial (i) and final (f) sites has been estimated in the framework of the standard Marcus–

Levich–Jortner theory as [64]

$$k_{if} = \frac{2\pi}{\hbar} V_{if}^2 \frac{1}{\sqrt{4\pi\lambda_s k_B T}} \sum_{n-0}^{\infty} \exp(-S) \frac{S^n}{n!} \times \exp\left[-\frac{(\Delta G^0 + \lambda_s + n\hbar\omega)^2}{4\lambda_s k_B T}\right] \quad (3)$$

with $k_B$ the Boltzmann constant and $T$ the temperature. $V_{if}$ is the transfer integral between the HOMO levels of the two interacting molecules, calculated here in a direct way at the semi-empirical Hartree–Fock INDO (intermediate neglect of differential overlap) level [65]. For all snapshots, the transfer integrals have been calculated for all pairs of adjacent molecules in a given layer (the values are vanishingly small for molecules located in different, even adjacent layers). $S$ is the Huang–Rhys factor defined as $S = \lambda_i/\hbar\omega$, with $\lambda_i$ the internal reorganization energy and $\hbar\omega$ the energy of an effective mode assisting the charge transfer (and $n$ the vibrational quantum number). $\lambda_i$ has been estimated in a previous study to be 97 meV for holes in pentacene [66] and $\hbar\omega$ set equal here to 0.2 eV (i.e., the typical energy for C–C bond stretching or aromatic ring breathing modes) so that $S = 0.485$. $\lambda_s$ is the external reorganization energy set equal to a reasonable value of 0.2 eV in both cases [67]. We stress that the choice of these values is not critical since it does not significantly affect the ratio of the mobility in the presence of the different dielectric layers that modulates the $\Delta G^\circ$ parameter. The latter is associated to the $\Delta E_{tot}$ parameter when neglecting entropy effects. The broadening parameter instantaneous values were found to be fairly constant in the nanoseconds and picoseconds time scales typical of a hopping event (see Fig. S2), therefore the $\Delta E_{diel}$ values have been averaged over the whole dynamics (Fig. 2). Interestingly, without averaging, the mobility values are vanishingly small due to the formation of deep trap levels. In a second stage, the transfer rates have been injected into a Monte–Carlo scheme to propagate a single charge in the various pentacene layers following a procedure detailed in Ref. [34]. If $d$ is the total distance traveled by the charge, $\tau$ the total time obtained from the inverse of the rates of all accepted jumps and $F$ the amplitude of the applied electric field (a typical value of $10^4$ V cm$^{-1}$ is used in our simulations), the mobility $\mu$ is ultimately obtained as

$$\mu = d/(\tau F) \quad (4)$$

## Acknowledgements

We acknowledge stimulating discussions with Prof. Paul Heremans (IMEC). The work in Mons is partly supported by the Belgian Federal Government ''Interuniversity Attraction Pole in Supramolecular Chemistry and Catalysis, PAI 5/3''; the European projects MODECOM (NMP3-CT-2006-016434; the European Community's Seventh Framework Programme (FP7/2007-2013) under grant agreement 212311 for the ONE-P project; and the Belgian National Fund for Scientific Research (FNRS/FRFC). J.C. and D.B. are FNRS Research Fellows; N.M. acknowledges a grant from the ''Fonds pour la Formation à la Recherche dans l'Industrie et dans l'Agriculture (FRIA)''. The work in Bologna is partly supported by the European projects MODECOM and ONE-P and by the Emilia–Romagna regional projects PRITT ''NANOFABER'' and ''PROMINER''. Supporting Information is available online from Wiley InterScience or from the author.

Received: June 18, 2009
Published online: September 1, 2009

[1] *Handbook of Conducting Polymers*, 3rd ed. (Eds: T. A, Skotheim, J. R. Reynolds), CRC Press, Boca Raton, FL **2007**.
[2] D. Braga, G. Horowitz, *Adv. Mater.* **2009**, *21*, 1473.
[3] S. Allard, M. Forster, B. Souharce, H. Thiem, U. Scherf, *Angew. Chem. Int. Ed.* **2008**, *47*, 4070.
[4] J. Zaumseil, H. Sirringhaus, *Chem. Rev.* **2007**, *107*, 1296.
[5] G. Horowitz, *Adv. Mater.* **1998**, *10*, 365.
[6] V. Coropceanu, J. Cornil, D. A. da Silva Filho, Y. Olivier, R. Silbey, J.-L. Brédas, *Chem. Rev.* **2007**, *107*, 926.
[7] V. Podzorov, E. Menard, A. Borissov, V. Kiryukhin, J. A. Rogers, M. E. Gershenson, *Phys. Rev. Lett.* **2004**, *93*, 086602.
[8] H. Bässler, *Phys. Status Solidi B* **1993**, *175*, 15.
[9] A. Troisi, *Adv. Mater.* **2007**, *19*, 2000.
[10] A. Troisi, G. Orlandi, *J. Phys. Chem. A* **2006**, *110*, 4065.
[11] A. Troisi, G. Orlandi, J. E. Anthony, *Chem. Mater.* **2005**, *17*, 5024.
[12] F. Dinelli, M. Murgia, P. Levy, M. Cavallini, F. Biscarini, D. M. de Leeuw, *Phys. Rev. Lett.* **2004**, *92*, 116802.
[13] J. Veres, S. D. Ogier, W. Leeming, D. C. Cupertino, S. M. Khaffaf, *Adv. Funct. Mater.* **2003**, *13*, 199.
[14] C. Kim, A. Facchetti, T. J. Marks, *Science* **2007**, *318*, 76.
[15] N. Benson, C. Melzer, R. Schmechel, H. von Seggern, *Phys. Status Solidi A* **2008**, *205*, 475.
[16] P. M. Borsenberger, J. J. Fitzgerald, *J. Phys. Chem.* **1993**, *97*, 4815.
[17] K. P. Pernstich, C. Glodmann, C. Krellner, D. Oberhoff, D. J. Gundlach, B. Batlogg, *Synth. Met.* **2004**, *146*, 325.
[18] J. Takeya, T. Nishikawa, T. Takenobu, S. Kobayashi, Y. Iwasa, T. Mitani, C. Goldmann, C. Krellner, B. Batlogg, *Appl. Phys. Lett.* **2004**, *85*, 5078.
[19] I. N. Hulea, S. Fratini, H. Xie, C. L. Mulder, N. N. Iossad, G. Rastelli, S. Ciuchi, A. F. Morpurgo, *Nat. Mater.* **2006**, *5*, 982.
[20] T. Richards, M. Bird, H. Sirringhaus, *J. Chem. Phys.* **2008**, *128*, 234905.
[21] J. F. Chang, H. Sirringhaus, M. Giles, M. Heeney, I. McCulloch, *Phys. Rev. B* **2007**, *76*, 205204.
[22] S. Verlaak, P. Heremans, *Phys. Rev. B* **2007**, *75*, 115127.
[23] D. H. Kim, H. S. Lee, H. Yang, L. Yang, K. Cho, *Adv. Funct. Mater.* **2008**, *18*, 1363.
[24] C. Kim, A. Facchetti, T. J. Marks, *Adv. Mater.* **2007**, *19*, 2561.
[25] A. Gerlach, S. Sellner, S. Kowarik, F. Schreiber, *Phys. Status Solidi A* **2008**, *205*, 461.
[26] L. L. Chua, J. Zaumseil, J. F. Chang, E. C. W. Ou, P. K. H. Ho, H. Sirringhaus, R. H. Friend, *Nature* **2005**, *434*, 194.
[27] M. H. Yoon, A. Facchetti, T. J. Marks, *Proc. Natl. Acad. Sci. USA* **2005**, *102*, 4678.
[28] F. Todescato, R. Capelli, F. Dinelli, M. Murgia, N. Camaioni, M. Yang, R. Bozio, M. Muccini, *J. Phys. Chem. B* **2008**, *112*, 10130.
[29] R. Berardi, L. Muccioli, C. Zannoni, *ChemPhysChem* **2004**, *5*, 104.
[30] G. Tiberio, L. Muccioli, R. Berardi, C. Zannoni, *ChemPhysChem* **2009**, *10*, 125.
[31] M. E. Gershenson, V. Podzorov, A. F. Morpurgo, *Rev. Mod. Phys.* **2006**, *78*, 973.
[32] M. P. Allen, D. J. Tildesley, in *Computer Simulations of Liquids*, Oxford University Press, Oxford, UK **1987**.
[33] C. Curutchet, G. D. Scholes, B. Mennucci, R. Cammi, *J. Phys. Chem. B* **2007**, *111*, 13253.
[34] Y. Olivier, V. Lemaur, J.-L. Brédas, J. Cornil, *J. Phys. Chem. A* **2006**, *110*, 6356.
[35] I. I. Fishchuk, A. Kadashchuk, H. Bässler, S. Nespurek, *Phys. Rev. B* **2003**, *67*, 224303.
[36] J. Cottaar, P. A. Bobbert, *Phys. Rev. B* **2006**, *74*, 115204.
[37] F. Castet, P. Aurel, A. Fritsch, L. Ducasse, D. Liotard, M. Linares, J. Cornil, D. Beljonne, *Phys. Rev. B* **2008**, *77*, 115210.
[38] D. T. Gillepsie, *J. Phys. Chem.* **1977**, *81*, 2340.
[39] D. T. Gillepsie, *J. Comput. Phys.* **1976**, *22*, 403.
[40] D. Andrienko, J. Kirkpatrick, V. Marcon, J. Nelson, K. Kremer, *Phys. Status Solidi B* **2008**, *245*, 830.
[41] J. Kirkpatrick, V. Marcon, J. Nelson, K. Kremer, D. Andrienko, *Phys. Rev. Lett.* **2007**, *98*, 227402.

[42] S. Athanasopoulos, J. Kirkpatrick, D. Martínez, J. M. Frost, C. M. Foden, A. B. Walker, J. Nelson, *Nano Lett.* **2007**, *7*, 1785.
[43] D. Frenkel, B. Smit, *Understanding Molecular Simulations: From Algorithms to Applications*, Academic, San Diego, CA, US **1996**.
[44] G. M. Day, T. G. Cooper, A. J. Cruz-Cabeza, K. E. Hejczyk, H. L. Ammon, S. X. M. Boerrigter, J. S. Tan, R. G. Della Valle, E. Venuti, J. Jose, S. R. Gadre, G. R. Desiraju, T. S. Thakur, B. P. van Eijck, J. C. Facelli, V. E. Bazterra, M. B. Ferraro, D. W. M. Hofmann, M. A. Neumann, F. J. J. Leusen, J. Kendrick, S. L. Price, A. J. Misquitta, P. G. Karamertzanis, G. W. A. Welch, H. A. Scheraga, Y. A. Arnautova, M. U. Schmidt, J. van de Streek, A. K. Wolf, B. Schweizer, *Acta Crystallogr. Sect. B* **2009**, *65*, 107.
[45] M. R. Wilson, *Int. Rev. Phys. Chem.* **2005**, *24*, 421.
[46] D. N. Theodorou, *Comput. Phys. Commun.* **2005**, *169*, 82.
[47] M. Praprotnik, L. Delle Site, K. Kremer, *Annu. Rev. Phys. Chem.* **2008**, *59*, 545.
[48] A. D. Mackerell, *J. Comput. Chem.* **2004**, *25*, 1584.
[49] M. J. Frisch, G. W. Trucks, H. B. Schlegel, G. E. Scuseria, M. A. Rob, J. R. Cheeseman, J. A. Montgomery, Jr, T. Vreven, K. N. Kudin, J. C. Burant, J. M. Millam, S. S. Iyengar, J. Tomasi, V. Barone, B. Mennucci, M. Cossi, G. Scalmani, N. Rega, G. A. Petersson, H. Nakatsuji, M. Hada, M. Ehara, K. Toyota, R. Fukuda, J. Hasegawa, M. Ishida, T. Nakajima, Y. Honda, O. Kitao, H. Nakai, M. Klene, X. Li, J. E. Knox, H. P. Hratchian, J. B. Cross, V. Bakken, C. Adamo, J. Jaramillo, R. Gomperts, R. E. Stratmann, O. Yazyev, A. J. Austin, R. Cammi, C. Pomelli, J. W. Ochterski, P. Y. Ayala, K. Morokuma, G. A. Voth, P. Salvador, J. J. Dannenberg, V. G. Zakrzewski, S. Dapprich, A. D. Daniels, M. C. Strain, O. Farkas, D. K. Malick, A. D. Rabuck, K. Raghavachari, J. B. Foresman, J. V. Ortiz, Q. Cui, A. G. Baboul, S. Clifford, J. Cioslowski, B. B. Stefanov, G. Liu, A. Liashenko, P. Piskorz, I. Komaromi, R. L. Martin, D. J. Fox, T. Keith, M. A. Al-Laham, C. Y. Peng, A. Nanayakkara, M. Challacombe, P. M. W. Gill, B. Johnson, W. Chen, M. W. Wong, C. Gonzalez, J. A. Pople, *Gaussian 03*, Gaussian, Inc, Wallingford, CT **2003**.
[50] A. Jakalian, B. L. Bush, D. B. Jack, C. I. Bayly, *J. Comput. Chem.* **2000**, *21*, 132.
[51] B. H. Besler, K. M. Merz, P. A. Kollman, *J. Comput. Chem.* **1990**, *11*, 431.
[52] W. D. Cornell, P. Cieplak, C. I. Bayly, I. R. Gould, K. M. Merz, D. M. Ferguson, D. C. Spellmeyer, T. Fox, J. W. Caldwell, P. A. Kollman, *J. Am. Chem. Soc.* **1995**, *117*, 5179.
[53] J. M. Wang, P. Cieplak, P. A. Kollman, *J. Comput. Chem.* **2000**, *21*, 1049.
[54] J. M. Wang, R. M. Wolf, J. W. Caldwell, P. A. Kollman, D. A. Case, *J. Comput. Chem.* **2004**, *25*, 1157.
[55] A. Soldera, N. Metatla, *Phys. Rev. E* **2006**, *74*, 061803.
[56] P. Procacci, T. A. Darden, E. Paci, M. Marchi, *J. Comput. Chem.* **1997**, *18*, 1848.
[57] M. Parrinello, A. Rahman, *J. Appl. Phys.* **1981**, *51*, 7182.
[58] U. Essmann, L. Perera, M. L. Berkowitz, T. Darden, H. Lee, L. G. Pedersen, *J. Chem. Phys.* **1995**, *103*, 8577.
[59] R. B. Campbell, J. M. Robertson, J. Trotter, *Acta Crystallogr.* **1962**, *15*, 289.
[60] T. Siegrist, C. Kloc, J. H. Schon, B. Batlogg, R. C. Haddon, S. Berg, G. A. Thomas, *Angew. Chem. Int. Ed.* **2001**, *40*, 1732.
[61] I. P. M. Bouchoms, W. A. Schoonveld, J. Vrijmoeth, T. M. Klapwijk, *Synth. Met.* **1999**, *104*, 175.
[62] C. C. Mattheus, A. B. Dros, J. Baas, G. T. Oostergetel, A. Meetsma, J. L. de Boer, T. T. M. Palstra, *Synth. Met.* **2003**, *138*, 475.
[63] R. G. Della Valle, E. Venuti, L. Farina, A. Brillante, *J. Phys. Chem. A* **2004**, *108*, 1822.
[64] J. Jortner, *J. Chem. Phys.* **1976**, *64*, 4860.
[65] A. Van Vooren, V. Lemaur, A. J. Ye, D. Beljonne, J. Cornil, *ChemPhysChem* **2007**, *8*, 1240.
[66] V. Coropceanu, M. Malagoli, D. A. da Silva Filho, N. E. Gruhn, T. G. Bill, J.-L. Brédas, *Phys. Rev. Lett.* **2002**, *89*, 275503.
[67] V. Lemaur, M. Steel, D. Beljonne, J.-L. Brédas, J. Cornil, *J. Am. Chem. Soc.* **2005**, *127*, 6077.